Design, fabrication, and characterization of circular Dammann gratings based on grayscale lithography

Uriel Levy,[1,*] Boris Desiatov,[1] Ilya Goykhman,[1] Tali Nachmias,[2] Avi Ohayon,[2] and Sheffer E. Meltzer[2]

[1]*Department of Applied Physics, The Benin School of Engineering and Computer Science, The Center for Nanoscience and Nanotechnology, The Hebrew University of Jerusalem, Jerusalem 91904, Israel*
[2]*Micro System and Smart Technologies, RAFAEL Ltd., P.O.B. 2250, Haifa 31021, Israel*
**Corresponding author: ulevy@cc.huji.ac.il*

Received December 14, 2009; revised February 3, 2010; accepted February 3, 2010;
posted February 19, 2010 (Doc. ID 121446); published March 15, 2010

We describe the design, fabrication, and experimental demonstration of a circular Dammann grating element generating a point-spread function of two concentric rings with equal intensity. The element was fabricated using grayscale lithography, providing a smooth and accurate phase profile. As a result, we obtained high diffraction efficiency and good uniformity between the two rings. © 2010 Optical Society of America

OCIS codes: 050.1950, 120.4610.

A Dammann grating, originally demonstrated by Dammann and Gortler [1], is a periodic structure that converts an incident laser beam into an array of output beams with equal intensities. Many designs of such gratings were introduced over the years, with the goal of maximizing the diffraction efficiency while keeping the uniformity as high as possible. The simplest designs make use of binary phase gratings [1,2]. Such gratings can generate a uniform array of spots, albeit with limited diffraction efficiency. More-advanced designs are based on multilevel phase gratings, allowing higher diffraction efficiency with a penalty of more challenging design, optimization, and fabrication process [3,4].

While most of the Dammann gratings generate a rectangular array of spots (either 1D or 2D), it is also possible to generate nonrectilinear spot arrays [5]. In particular, circular Dammann gratings (CDGs) are of interest owing to their circular symmetric point-spread function (PSF). Such gratings generate a set of concentric rings with equal intensity and thus can be integrated into many optical systems that also possess circular symmetry. So far, few CDGs were designed and demonstrated, all based on a binary phase profile [6,7], therefore having limited diffraction efficiency. In this Letter, we report on the design, fabrication, and experimental characterization of CDGs with multilevel phase profile that is implemented by the use of grayscale lithography and enables the achieving of high uniformity and diffraction efficiency.

In designing a CDG, we are seeking to find a phase function that will produce a desired diffraction pattern in the far field, or at the backfocal plane of a lens (assuming plane-wave illumination).

The CDG comprises a periodic phase function along the radial coordinate r. Therefore, using the thin-element approximation, the field at the exit plane of the CDG can be expanded in Fourier series, i.e.,

$$u_{in}(r) = C_0 + 2\sum_{n=1}^{\infty} C_n \cos\left(2\pi\frac{n}{\Lambda}r\right), \quad (1)$$

where Λ is the period of $u_{in}(r)$ along the radial coordinate. At the output plane, located at the backfocal plane of a lens, the field is proportional to the Fourier transform of $u_{in}(r)$, and thus is given by

$$u_{out}(\rho) = C_0\frac{1}{\pi|\rho|}\delta(\rho) + \frac{2}{\sqrt{\pi}}\sum_{n=1}^{\infty} C_n\frac{n/\Lambda}{(n/\Lambda+\rho)^{3/2}}\delta^{(1/2)}\left(\frac{n}{\Lambda}-\rho\right), \quad (2)$$

where $\delta^{(1/2)}$ is the half-order derivative of the Dirac delta function and ρ is the radial coordinate at the output plane [8].

As can be seen, the field at the output plane is composed of concentric rings, each having intensity proportional to

$$I_n \propto \left| C_n\frac{n/\Lambda}{(n/\Lambda+\rho)^{3/2}}\delta^{(1/2)}\left(\frac{n}{\Lambda}-\rho\right)\right|^2. \quad (3)$$

Using the relation $\delta^{(1/2)}(x) = -1/2\sqrt{\pi}1/x^{3/2}\mathrm{step}(x)$, where step$(x)$ is the unit step function, one can notice that I_n can be neglected for $\rho \neq n/\Lambda$. Therefore the intensity of each ring is proportional to $I_n \propto |C_n n/\Lambda/(2n/\Lambda)^{3/2}|^2 = C_n^2\Lambda/8n$. From the last expression it is clear that obtaining multiple concentric rings with equal *intensity* is possible by satisfying the relation $C_n = A\sqrt{n}$ (where A is a constant), whereas obtaining multiple concentric rings with equal *energy* is possible by satisfying the relation $C_n = B$, where B is a constant. This is because the energy is the result of multiplying the intensity of each ring by its area, which is proportional to the ring radius, whereas the radius in turn is proportional to n.

The goal of this paper is to design a CDG with a PSF comprising two concentric rings having equal intensity. Specifically, we designed our CDG to generate the rings along the first and the third diffraction orders. Thus the goal is to maximize C_1 and C_3, while diminishing all other C_N coefficients ($N \neq 1,3$). By optimizing the phase profile of the CDG, we were able to find a design providing both a perfect uniformity (i.e., $C_1 = C_3/\sqrt{3}$) and a high diffraction efficiency ($\sim$78% of the energy is contained within the two concentric rings). This design was obtained by expressing the phase function as a third-order polynomial equation, $\varphi(r) = [a_1 r + a_2 r^2 + a_3 r^3]2\pi$, where $\varphi(r)$ is the phase of $u_{in}(r)$. The transverse vector r is given in pixel units. We allocated 16 pixels per period; i.e., r is bounded between 1 and 16. Yet, to ensure zero energy at the central lobe and to eliminate the even diffraction orders, we have chosen an antisymmetric mirror symmetry by dividing the period into two halves, where the second half repeats the first half, with an addition of a π phase shift. By optimization, we found the coefficients to be $a_1 = 0.0688$, $a_2 = 0.0078$, and $a_3 = 0.0013$. The obtained phase function was replicated 12 times, ensuring large separation between the concentric rings. The predicted PSF of the CDG was obtained by calculating the Fourier transform of the above-mentioned phase function. A 2D intensity image of the calculated PSF is shown in Fig. 1(a). Figure 1(b) shows an intensity cross section along the center of Fig. 1(a). The two concentric rings can be clearly observed in both images. An additional ring corresponding to the fifth diffraction order can also be noticed, albeit with much lower intensity.

Based on the design described above, we fabricated a CDG in silicon using grayscale lithography [9,10]. The device was designed to operate around 1550 nm wavelength. Thus the etching depth for achieving 2π phase modulation is $h = \lambda/(n_s - 1) \approx 620$ nm, where $n_s = 3.48$ is the refractive index of silicon. First, a grayscale photomask was fabricated (Canyon Materials, Inc.) by electron-beam lithography on a high-energy beam-sensitive glass. The gray levels in the mask were determined by a calibration curve that allocates a gray-level value to each phase level, based on the calibrated fabrication process. We set the width of each ring (each gray level/phase value) to be 44.5 μm. Having 16 gray levels per period, the period size was set to 712 μm. We repeated this pattern 12 times along the radial coordinate. This results in a CDG diameter of 17 mm. Next, the pattern was transferred into a photoresist (PR) (AZ4533). The initial thickness of the PR was 1.6 μm. After exposure, the difference between the highest and the lowest PR thickness was 1.32 μm, because the maximal gray level is not fully opaque. Finally, the pattern was transferred to silicon by using reactive ion etching process based on a CF_4–O_2 chemistry. For the purpose of grayscale lithography we developed an etching process with a low selectivity ($\sim$0.45) and a low etching rate ($<$30 nm/min) such that the pattern can be accurately transferred from the resist to the silicon, with a height shrinking factor of $1/0.45 = 2.2$. Therefore the PR thickness of 1.32 μm was mapped to a thickness of $\sim$600 nm in the silicon substrate, which is close to the desired value. A color map image based on an optical profilometer (wyko NT9300, Veeco) measurement of the fabricated device is shown in Fig. 2.

To experimentally validate the operation of our CDG, it was placed in front of a 50 cm focal length lens and was illuminated by a collimated light from a diode laser source at a wavelength around 1.55 μm. The results were recorded by an InGaAs CCD camera (Indigo Alpha NIR) that was placed at the backfocal plane of the lens. A schematic drawing of the experimental setup is shown in Fig. 3.

The image captured by the CCD camera is shown in Fig. 4(a). A central cross section of the image is given in Fig. 4(b). The experimental results show very good agreement with the computer simulations. The high uniformity can be clearly observed. The observable central spot is an indication for nonvanishing dc term in the Fourier series. Yet it has a negligible effect on the diffraction efficiency, because, unlike 1D Dammann gratings, the energy at each or-

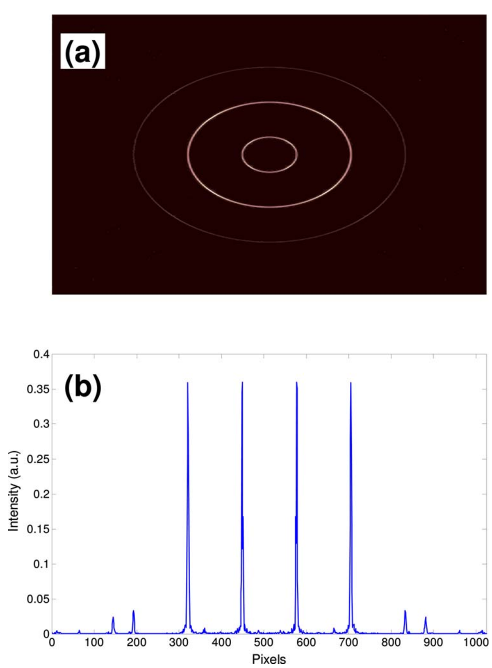

Fig. 1. (Color online) Simulation results showing the predicted intensity pattern in the far field: (a) 2D image, (b) intensity cross section across the center of (a).

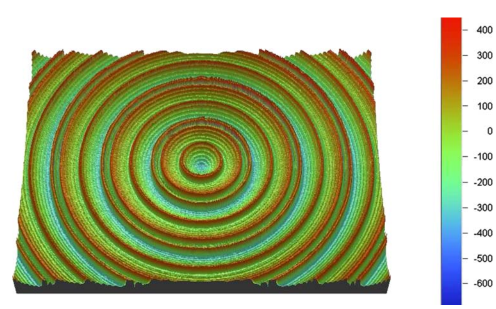

Fig. 2. (Color online) Optical profilometer color map image showing the central section of the fabricated CDG. The color scale represents height in nanometers.

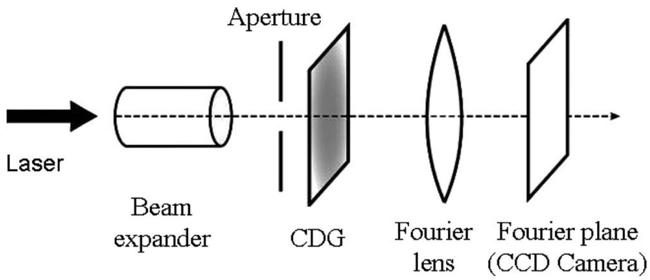

Fig. 3. Schematic diagram of the experimental setup.

der of the CDG is linearly proportional to its distance from the center. In addition, one may also notice the existence of a second order (an additional circular ring between the two designed rings). This may be the result of a slight deviation of the obtained phase profile from the designed phase profile. Such a discrepancy can be explained by a slight error in the phase-calibration process. Nevertheless, the intensity of this ring (after subtracting the camera noise) is ~15 times smaller than that of the major rings (first and third orders), thus having a negligible effect on the obtained result. An additional ring corresponding to the fifth diffraction order can also be observed. The intensity of this ring was measured to be ~10 times smaller than that of the major ring, which is in very good agreement with the computer simulations. Higher diffraction orders were very faint. Neglecting the zero-order term, the diffraction efficiency of our CDG is given by

$$\eta = \frac{I_1 2\pi R_1 + I_3 2\pi R_3}{\sum_{n=1}^{\infty} I_n 2\pi R_n}, \tag{4}$$

where I_n is the measured intensity of the nth diffraction order and R_n is the radius of the nth ring, satisfying $R_n = nR_1$. Based on Eq. (4), we found the diffraction efficiency to be 63%. To capture the higher diffraction orders we used a lens with shorter focal length of 10 cm. The obtained diffraction efficiency is lower than the simulated result. The major reason for this discrepancy is the existence of high diffraction orders. Although these orders have nearly negligible intensity (~15 times smaller than the intensity of the major rings), they carry nonnegligible energy because of their large perimeter, which is proportional to their radius. Therefore the effect of the high diffraction orders cannot be neglected, in contrast to a standard 1D Dammann grating. Another issue to be mentioned is the stray light. To account for this effect we also calculated the diffraction efficiency using integration over the intensity of the first and third rings and normalized this result by the overall measured power in the CCD camera. This approach resulted in ~58% diffraction efficiency, because the scattered light between diffraction orders is now being considered as well.

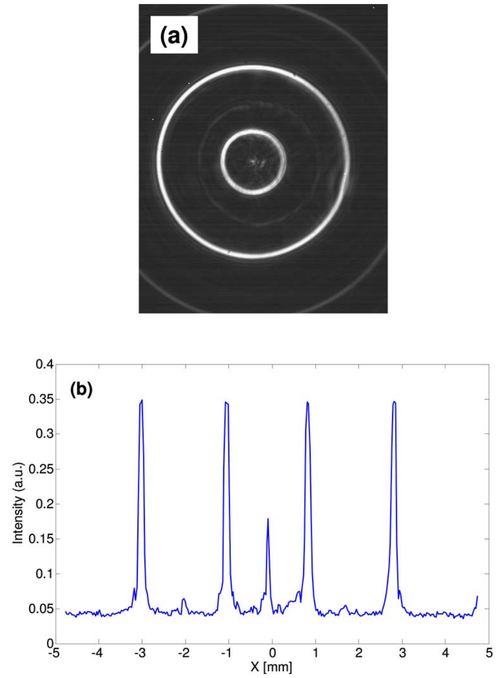

Fig. 4. (Color online) Experimental results showing the obtained intensity pattern in the far field: (a) 2D, (b) intensity cross section across the center of (a).

In summary, we demonstrated a circular Dammann grating that generates two concentric rings with equal intensity in the Fourier plane. The grating was fabricated using a grayscale lithography process, thus having a high uniformity and high diffraction efficiency. Such gratings can be used for the control of the PSF in circular symmetric optical systems.

References

1. H. Dammann and K. Gortler, Opt. Commun. **3**, 312 (1971).
2. H. Dammann and E. Klotz, Opt. Acta **24**, 505 (1977).
3. J. N. Mait, J. Opt. Soc. Am. A **7**, 1514 (1990).
4. S. J. Walker and J. Jahns, J. Opt. Soc. Am. A **7**, 1509 (1990).
5. N. Streibl, J. Mod. Opt. **36**, 1559 (1989).
6. C. Zhou, J. Jia, and L. Liu, Opt. Lett. **28**, 2174 (2003).
7. S. Zhao and P. S. Chung, Opt. Lett. **31**, 2387 (2006).
8. I. Amidror, J. Opt. Soc. Am. A **14**, 816 (1997).
9. M. LeCompte, X. Gao, and D. W. Prather, Appl. Opt. **40**, 5921 (2001).
10. M. Iqbal, T. Dillon, M. J. McFadden, D. Prather, and M. W. Haney, in *Frontiers in Optics*, OSA Technical Digest Series (Optical Society of America, 2005), paper JTuC24.